37p.

N62-16504

NASA TN D-1398

NASA TN D-1398

TECHNICAL NOTE

D-1398

A STUDY OF THRUST VECTOR STEERING FOR RENDEZVOUS WITH A NEAR-EARTH SATELLITE UTILIZING A THREE-STAGE VEHICLE LAUNCHED OUT OF THE SATELLITE PLANE

By Charles P. Llewellyn

Langley Research Center
Langley Station, Hampton, Va.

NATIONAL AERONAUTICS AND SPACE ADMINISTRATION

WASHINGTON October 1962

N62-16564

NATIONAL AERONAUTICS AND SPACE ADMINISTRATION

TECHNICAL NOTE D-1398

A STUDY OF THRUST VECTOR STEERING FOR RENDEZVOUS WITH A NEAR-EARTH SATELLITE UTILIZING A THREE-STAGE VEHICLE LAUNCHED OUT OF THE SATELLITE PLANE

By Charles P. Llewellyn

SUMMARY

A study of the problem of direct rendezvous with a near-earth satellite for the case where the ferry vehicle is launched out of the satellite plane has been made. This investigation was concerned with the efficiency of steering the ferry vehicle's velocity vector into the satellite plane at burnout by properly turning the main thrust vector during a portion of the power-on ascent trajectory. A typical three-stage booster system was utilized with the thrust steering employed only during the third-stage phase of the ascent. For the two techniques of thrust vector steering considered, which were essentially: (1) a slow constant turning of the thrust vector in the lateral direction during third-stage burning and (2) a turn of the thrust vector in the lateral plane just prior to third-stage ignition and holding the direction fixed in inertial space, it was found that the cost in terms of the idealized velocity increment ΔV required after third-stage burnout to effect final rendezvous was very nearly the same. The total cost of the maneuver was critically dependent on the cross-plane angle ψ_V that remained at burnout and the minimum ΔV was obtained when this angle approached zero. It was found that for these cases where the angle was nearly zero the velocity losses incurred (and hence the ΔV required for rendezvous) as a result of the thrust vector steering were approximately 400 feet per second and 1,600 feet per second for the initial offsets of 2° and 4°, respectively. The methods used in this investigation were compared with the "adjacency" technique and were found to be more efficient.

INTRODUCTION

Development of a rendezvous capability is an important consideration in future space exploration. Many uses of rendezvous have been envisioned including such operations as space station maintenance, assembly of orbital units for lunar and interplanetary missions, personnel transfer and rescue. One of the most attractive advantages offered by orbital rendezvous is the potentiality of performing many space missions with relatively small launch vehicles. In keeping with this, present-day booster systems can be utilized for space operations while the next generation of launch vehicles is being developed.

From the standpoint of efficiency and guidance simplicity, it is desirable to launch the rendezvous vehicle when the launch site is in the orbital plane of the satellite. However, in order to provide a practical launch frequency capability (for example, once a day) and to account for possible launch time uncertainties due to hold times on the pad, launches from out of the satellite's orbital plane will generally be required. Several solutions for out-of-plane launch and rendezvous are discussed in references 1 and 2. Reference 1 shows the losses that occur, based on a two-impulse plan, as a result of out-of-plane launches. Reference 2 presents a scheme where the ferry vehicle is launched out of the satellite plane so that at injection it is adjacent to the target but not in the same plane. Rendezvous is accomplished at the nodal point of the two orbits where the ferry's direction is changed to coincide with that of the satellite.

An investigation of the direct rendezvous, out-of-plane launch, using finite burning times is presented in this paper. In particular, this study examines the launch trajectory of a typical present-day booster system to determine whether during the latter portion of the main power-on ascent a reasonably efficient turn can be made into the desired orbital plane such that at burnout the final correction required to rendezvous will be minimized. The investigation does not attempt to optimize the turn maneuver nor generalize for any arbitrary offset condition and satellite altitude but merely shows the feasibility and additional cost of such a maneuver for two example cases.

SYMBOLS

A	transformation matrix
C_D	drag coefficient
D	drag, subscripts denote appropriate component, lb
d	offset distance, ηr, ft
g_e	gravity at earth's surface, ft/sec^2
H_0	initial azimuth heading of thrust axis (0° due north, 90° due east, etc.), deg

i_s inclination of target orbit, deg

l,m,n elements of transformation matrix

m vehicle mass, slugs

r radial distance from earth center to present position of vehicle's center of mass, ft

r_e earth radius, ft

R,T,N left-handed axis system oriented at vehicle's present position with R-axis positive radially outward from earth center and the T-axis positive in direction of motion and lying in present position plane (See fig. 1.)

S reference area, sq ft

t time, sec

$\overline{T}$ thrust, subscripts denote appropriate component, lb

ΔV idealized velocity increment, ft/sec

V velocity, subscripts denote appropriate component, ft/sec

V_a relative velocity, subscripts denote appropriate component, ft/sec

V_c circular satellite velocity, ft/sec

V_e rotational velocity of position assuming present position rigidly attached to the earth, ft/sec

V_f final inertial velocity, altitude corrected, ft/sec

W weight, subscripts denote appropriate component, lb

x,y,z inertial right-handed system of axes fixed at earth's center oriented such that the positive z-axis passes through the nodal point of target plane and the positive y-axis points north and is axis of rotation of earth (See fig. 1(a).)

x_B,y_B,z_B right-handed set of body axes centered at origin of R,T,N system of axes, x_B-axis positive in direction of motion and y_B-axis positive in direction of positive N-axis and lying in T,N plane

ρ	atmospheric density, slugs/cu ft
δ	angle at present position, in T,N plane, between present position and a parallel of latitude (positive when T-axis is north of parallel of latitude), deg (See fig. 1(b).)
ζ	angle at present position between appropriate velocity vector and T,N plane, subscript denotes the velocity vector, deg (See fig. 1(b).)
η	angular offset measured along meridian between target plane and present position, $\theta_p - \theta$, deg (See fig. 1(a).)
θ	angle along meridian between equatorial plane and present position (analogous to latitude), positive in northern hemisphere, negative in southern hemisphere, deg
θ_p	angle along meridian passing through present position between equatorial plane and target plane, deg (Same sign convention as θ.)
θ_T	angle between thrust vector $\overline{T}$ (x body axis) and the T,N plane, positive when thrust vector lies above T,N plane, deg (See fig. 1(b).)
ϕ	inertial range angle measured from initial inertial position to present inertial position, deg
ψ	angle at present position in T,N plane between T-axis and projection of appropriate velocity vector onto T,N plane. Subscripts denote appropriate velocity vector, deg (See fig. 1(b).)
ψ_T	angle measured in horizontal T,N plane between T-axis and projection of thrust vector onto the T,N plane, deg (See fig. 1(b).)
Ω	angle measured in equatorial plane from nodal point of target plane to projection of present position onto equatorial plane, deg
ω_e	angular rate of earth rotation, radians/sec
ω_{y_B}	angular rate about y body axis, deg/sec
ω_{z_B}	angular rate about z body axis, deg/sec

Subscript:

0 denotes conditions at t equal to zero

A dot over a symbol indicates differentiation with respect to time.

PROBLEM DESCRIPTION

The following investigation is concerned with direct rendezvous between a near-earth satellite and a vehicle launched from the earth but not in the same plane as the orbiting satellite. In particular, an examination is made of the ascent trajectory of a ferry vehicle to determine whether an intelligent and reasonably efficient turn of its velocity vector into the satellite plane can be effected during the latter portion of the main power-on boost.

The problem investigated was, with a given launch vehicle system and a given offset distance, to arrive at some point in space lying in the plane of a target orbit with conditions such that at burnout the ideal velocity correction ΔV required for final rendezvous maneuver was minimized (see sketch 1).

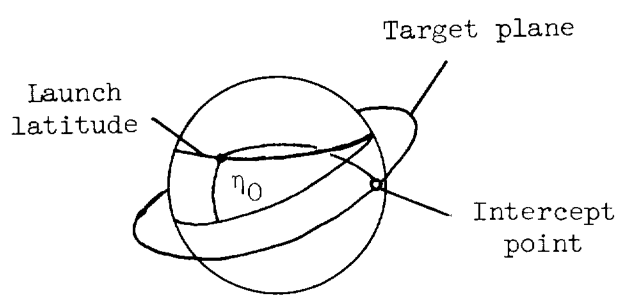

Sketch 1

That is, a launch trajectory was desired which placed the ferry vehicle at burnout near the apogee of the ascent, at the satellite altitude, and in the satellite plane. No "over and down" rendezvous paths were considered and further, no consideration was given trajectories wherein the vehicle coasted to the desired conditions after final stage burnout. A three-stage launch system was selected where the total flight time and stage ignition times of the vehicle were held fixed. The magnitude of the problem was somewhat reduced by restricting the ferry vehicle to no maneuvering during the first two burning stages and to two turning techniques. Different launch headings were considered which resulted in only small variations in the time histories of the first two stages.

An intuitive feeling for this problem may be obtained by referring to sketches 1 and 2. Sketch 2 shows offset distance d plotted against flight time.

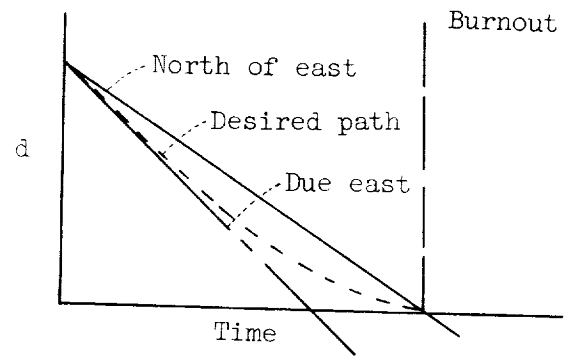

Sketch 2

The first concern was that of obtaining intercept with the target plane at the proper time (that is, at burnout with offset distance equal to zero). The target plane was assumed to have been established by launching into a circular orbit, due east from some latitude in the northern hemisphere. The ferry vehicle was launched from the same latitude but because of the rotation of the earth was offset from the target plane by some angle. For the offset angles considered (4° or less) and relatively small range angles traversed by the ferry vehicle from launch to burnout (about 20°), a due east launch with no lateral turning will intercept the target plane prior to burnout as depicted in sketch 2. Also as shown in this sketch, there is some launch heading north of east such that, again with no turning, the target plane will be intercepted at burnout. For this case then, if it is assumed that the ferry vehicle would be at the proper altitude with its velocity nearly horizontal, the ideal final rendezvous maneuver would consist of adding a velocity correction such that the resultant would be equal to the satellite velocity and would lie in the satellite plane. As might be expected, "turning the corner" at this point is expensive. As mentioned in the initial statement of the problem, the object was not only to arrive in the satellite plane at burnout but also with conditions such that the velocity correction required for the final rendezvous maneuver was minimized. An obvious approach is reduction of the angle or "corner" that the velocity vector must be turned through at burnout to place the final velocity into the satellite plane. Reference back to sketch 2 shows the desired path which, as depicted, arrives at the burnout point tangent to the satellite plane with no angle correction required. In order to effect such a path, however, the thrust of the ferry vehicle during the ascent trajectory must be directed laterally relative to its velocity. This procedure will obviously result in velocity losses as compared with the no-turn case. These velocity losses will likewise have to be made up in the final rendezvous maneuver.

The determination of the nature of the turning maneuvers required during the power-on ascent trajectory and their cost in terms of the final ΔV (ideal) required for rendezvous for two initial offset values is the basis of this paper.

VEHICLE DESCRIPTION AND PROBLEM CONDITIONS

The launch vehicle chosen for this investigation was a three-stage configuration assumed to be capable of placing approximately 12,000 pounds of payload into a 122-nautical-mile circular orbit. The thrust profile is presented in figure 2. Also included on the figure are the staging times. The first- and second-stage propellant was LOX/RP and the third-stage propellant was LOX/H_2.

The basic launch trajectory, a due east launch heading from a latitude of 28.5°, was established by programing the vehicle pitch attitude such that the vehicle rose vertically for 15 seconds, executed a pitch-over maneuver, followed thereafter by a gravity turn (zero lift) to burnout of the first stage. Constant pitch-rate commands were used during second- and third-boost stages. The vehicle payload was sized so that nearly circular orbital conditions existed at third-stage burnout. The great-circle range angle from the launch site to the injection point was about 19.7°. The inertial velocity, flight-path angle, altitude, and time histories are shown in figure 3. The basic launch trajectory used to establish the target orbit was also the base trajectory for the out-of-plane launches modified to include the required turn maneuvers.

The same launch site was used for all cases. The offset angles were generated by considering the launch to occur before the launch site rotated into the target plane. The cases where the same values of offset angles could be generated by launching the ferry vehicle after the launch site had rotated under the target plane were not considered in this investigation. It is felt, however, that the same problems and philosophies used in the present investigation would be applicable to this case, with only minor program changes.

The particular values of offset used in this study were 2° and 4°. These values were considered to be reasonable in that they allow for hold times from about $1\frac{1}{2}$ to $2\frac{1}{4}$ hours, respectively, and also give a considerable margin for insuring at least a once-a-day capability.

PROCEDURES

Two techniques were considered for steering the thrust vector laterally so that the velocity vector was turned in the proper direction. In both cases the thrust vector was assumed to be fixed along the ferry vehicle's longitudinal axis and was controlled laterally by introducing into the equations of motion an angular rate ω_{z_B} about the body yaw axis. The thrust attitude with respect to the local horizontal was programed to be the same in all cases. The actual thrust control equations are presented in the appendix (eqs. (A28) and (A29)). The two methods have been designated by the manner in which the thrust vector was steered laterally during third-stage burning and will be referred to as the constant-rate method and the fixed-direction method. In the constant-rate method the thrust vector was rotated by using a relatively small constant value of turn rate during the entire third-stage portion of the ascent. The fixed-direction method consisted of setting the thrust vector off in the yaw plane by commanding a relatively larger rate for 1 second prior to third-stage ignition (during second-stage coast) and then holding this direction fixed in inertial space by assuming zero turn rate throughout third-stage burning. Whereas either of these maneuvers would appear to be feasible in a practical situation, both were considered in the calculations to determine whether possibly one was more efficient than the other. For example, in the constant-rate method, it was reasoned that by rotating the thrust vector slowly the velocity vector would follow the thrust, keep the angle between the two comparatively small, and thus maintain a reasonable degree of thrusting efficiency. On the other hand, the fixed-direction method attempts to turn the velocity vector earlier in the ascent, the philosophy here being that the maneuvering would take place where the magnitude of the velocity vector would be lower than in the constant-rate method. As was noted in the introduction, the attempt here was not to cover every possible maneuver which could be applied to accomplish this task. It is reasonable to suspect that, in the practical and/or in the closed-loop situation, a combination of the two techniques would actually be employed.

As mentioned previously, there is one initial heading for a particular value of offset that will arrive at the proper point in space with no turning or maneuvering. This case, referred to hereafter as the straight-in shot is used as a common point for the two techniques. Starting then with this case, various combinations of launch heading and thrust turning rate were investigated. It should also be pointed out here that for a given initial heading there is only one turn rate per technique which will arrive at the proper point in space. The runs were evaluated on the basis of the ideal impulsive velocity ΔV required at burnout to bring the ferry vehicle up to circular satellite velocity and at the same time rotate its velocity vector V_f so that it will coincide with that of the satellite. From the following sketch, it can be seen that this quantity may be computed by the expression

$$\Delta V = \left(V_c^2 + V_f^2 - 2V_cV_f \cos \zeta_V \cos \psi_V\right)^{1/2}$$

where V_f is the ferry velocity at burnout, V_c is the circular satellite velocity, and ζ_V and ψ_V are the vertical and lateral angles, respectively, that V_f makes with V_c.

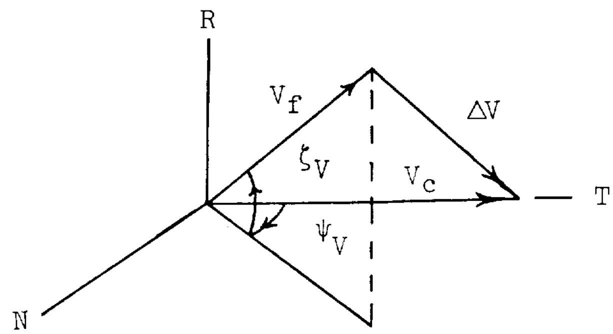

Sketch 3

In some cases, because of the rather severe turn maneuver employed, the reduction in altitude from the no-turn case became significant. This loss in altitude is attributed primarily to the fact that part of the vehicle thrust is required to turn the velocity vector laterally during the ascent and therefore the performance (final velocity and altitude) based on the no-turn case is certain to be degraded. This altitude difference is important since, in order to recover this loss to effect rendezvous, the vehicle's velocity will be reduced. Several runs were made wherein the vehicle's pitch program was adjusted such that the altitude loss was regained. Rather than iterating for every case where this loss was significant, an estimate was obtained for the two techniques of the altitude correction required in terms of a ΔV per nautical mile. This correction was estimated to be 23.3 feet per second per nautical mile and 17.5 feet per second per nautical mile for the constant-rate and the fixed-direction methods, respectively. These corrections were applied to the burnout velocity for the few cases where the altitude loss at third-stage burnout was greater than 1/2 nautical mile.

RESULTS AND DISCUSSION

The results of this investigation are presented in figures 4 to 8 and table I. Figures 4 to 7 are plots of the offset distance in feet against time. Figure 8 and table I summarize the cases investigated in terms of the velocity corrections required for final rendezvous. The launch headings and turning rates for the cases are indicated on the appropriate figures. In figures 4 to 7 it should be noted that only the third-stage burning portion of the ascent trajectory is presented. As mentioned previously, all the maneuvering takes place during this portion of the flight and thus is the primary area of interest. Further, all the trajectories were essentially the same through second stage, differing only slightly due to the initial launch heading.

Figure 4 presents the straight-in (no turn) shots for $\eta_O = 2^{\circ}$ and 4°. The initial (launch) headings measured from north required and the ΔV required for rendezvous for the two values of initial offset angles are noted. These two time histories are not straight lines since the vehicle is thrusting and hence the closure rate (offset rate) between the two planes increases with time. The ΔV required to rendezvous for these two cases is almost entirely that necessary to correct for the lateral angle ψ_V remaining at burnout. (See table I.)

To decrease the ψ_V at burnout, runs were made wherein the vehicle was launched more easterly than for these cases and then turned north of east by properly steering the thrust vector. A set of the offset-distance time histories for these cases is shown in figure 5(a) for $\eta_O = 2^{\circ}$ for the constant-rate method (fig. 5(a)) and in figure 5(b) for the fixed-direction method. The case numbers, launch headings, thrust-vector turn rates, and the ΔV required for rendezvous are noted on the figure. It should be pointed out again that the ω_{z_B} shown for the fixed-direction method is held for only 1 second. Also included for comparison on these plots is the straight-in shot. The value of offset distance at third-stage ignition is directly dependent on the launch heading and for this figure varies from about 590,000 feet for the straight-in shot to about 470,000 feet for the range of headings investigated. Notice in this figure that, as the heading angle is increased, the turn rate required for intercept at burnout must also increase as would be expected. The bottom curves of figures 5(a) and 5(b) are the time histories for the proper combination of thrust steering and initial heading that result in essentially zero ψ_V at burnout. The smallest possible ψ_V at burnout is intuitively desirable since cross-plane errors are minimized.

A set of offset-distance time histories for $\eta_0 = 4^\circ$ is presented in figure 6(a) for the constant-rate method and in figure 6(b) for the fixed-direction method. In figure 6, as in figure 5, the case number, initial launch heading, thrust-vector turn rate, and the ΔV required for rendezvous are noted on the figures for each of the curves. Also included in figures 6(a) and 6(b) is the straight-in shot. The range of offset distance at third-stage ignition due to initial heading for the cases considered in this figure is from about 1.2×10^6 feet to about 0.98×10^6 feet. As was noted on figure 5, as the initial heading is increased, so is the turn rate required for intercept.

Figure 7 presents the best cases for the two steering methods and the two offset conditions investigated. Figures 7(a) and 7(b) are for the 2° and 4° offsets, respectively. Noted on this figure are the case numbers, initial launch headings, the turn rates required, the cross-plane angle ψ_V, and the ΔV required to rendezvous. The straight-in shot is also included in this figure. The term "best" does not imply the optimum, but rather for the turn maneuver employed, the cross-plane errors were minimized and hence the ΔV values required to initiate final rendezvous were minimized. As can be seen from this figure, the ferry vehicle intercepts the target plane nearly tangent for both methods and approaches the desired path discussed previously. It should be noted in table I that, for these cases, where the ψ_V was near zero, the velocity required is almost entirely due to the losses incurred in steering the ferry vehicle, that is, the ΔV required is essentially that required to bring the ferry vehicle up to orbital velocity.

For the 2° offset cases the reduction in burnout velocity due to lateral thrust vector steering was approximately 360 feet per second for both turning techniques or about 3 percent of the velocity added during third stage. For the 4° offset cases, this reduction in burnout velocity was approximately 1,500 feet per second for the two turning techniques. This value amounts to slightly less than 10 percent of the velocity added during third stage and is about four times that required for the 2° offset cases.

Although no analytical solution was found that would give the amount of thrust steering required for a given initial heading, or combination of initial heading and turn rate that would give the most efficient maneuver subject to the problem constraints, after a few initial runs, a useful set of sensitivity parameters was obtained. These relationships were in the form of a sensitivity of offset distance to initial heading and turn rate and reduced considerably the number of runs required for a given series. These parameters are listed in the following table and were found to be independent of initial offset angle η_0.

Parameter	No turn $(\eta_0 = 2^o, 4^o)$	Constant-rate method $(\eta_0 = 2^o, 4^o)$	Fixed-direction method $(\eta_0 = 2^o, 4^o)$
$\Delta d_{B.O.}/\Delta H_0$	2.015×10^5	-----------	-----------
$\Delta d_{B.O.}/\Delta\omega_{z_B}$	-----------	0.544×10^7	0.408×10^5

Figure 8 and table I summarize the results obtained in this study. Figures 8(a) and 8(b) present the cost in terms of the ΔV required to initiate final rendezvous for both steering techniques and the two offset conditions. The range of ΔV values for the two offsets are from about 2,500 feet per second to 413 feet per second for the 2^o offset and from about 5,000 feet per second to 1,600 feet per second for the 4^o offset. In both figures 8(a) and 8(b) the curves begin with the straight-in or no-turn case and terminate with the cases where the proper combination of initial heading and turn rate resulted with interception occurring at burnout with ψ_V approximately equal to zero. As can be seen from table I the smallest ΔV for both turning methods was obtained for those cases where the ψ_V at burnout was essentially zero. As was pointed out earlier, for a given initial heading there is only one turn rate per technique that will satisfy the end condition of intercept at burnout. It also follows that there is only one combination of initial heading and turn rate that will give the desired path, that is, intercept at burnout with ψ_V equal to zero. Increasing the heading angles and turn rates beyond the values indicated would result in the final ψ_V becoming negative. Not only would these trajectories intercept the target plane twice (once prior to burnout and then again at burnout) but they would obviously be more expensive than the cases where $\psi_V = 0$. Aside from the fact that the angles would be finite, the velocity losses due to steering would also be greater for a negative ψ_V than for a positive ψ_V, since as has been shown, as the initial heading angles and turn rates are increased, the burnout velocity decreases. This was the reason for terminating the runs and curves with the $\psi_V \approx 0$ cases.

Reference to table I and figure 8 shows that ΔV is highly sensitive to the ψ_V at burnout, more so than to the velocity losses incurred during steering. As to which steering method is the best, from the results indicated on this figure, there appears to be little difference between the two as the desired path is approached, the difference being only about 50 feet per second for the 2^o offset and about 150 feet per second for the 4^o offset cases.

In an attempt to compare the methods of this study with the "out-of-plane adjacency" method discussed in reference 2, a ΔV was computed based on that technique by using the offset conditions of this study. Here the launch site is out of the target plane and the ferry vehicle is launched so that at injection it is adjacent to the target at the same velocity and altitude, the velocity vectors being roughly parallel but in different orbital planes. At the nodal point of the two orbits (approximately 90° later) a ΔV is added so that the ferry's velocity direction is made to coincide with that of the target. For a nonrotating earth, if the ferry vehicle is launched at the offsets used in this study (2° and 4°), then at burnout the vehicle will be in an orbit that has a difference in inclination from the target orbit that depends on the particular values of η_O. For the 2° offset this difference is about 2.1° and for the 4° offset this difference is about 4.4°. If the vehicle is then allowed to coast until the two planes intersect (approximately 90°), the angle between the two planes (in this case ψ_V) will also be the difference in inclinations. The ΔV required using this method was found to be about 930 feet per second for the 2° offset and about 1,960 feet per second for the 4° offset and is indicated on the figure by the square symbol.

CONCLUDING REMARKS

This study of the direct-rendezvous out-of-plane launch utilizing finite burning times indicates that a reasonably efficient turn maneuver can be executed during the main portion of the power-on ascent. Two thrust vector steering techniques were examined, a constant-rate method and a fixed-direction method. It was found that the most efficient cases, from the standpoint of the minimum ΔV required to initiate final rendezvous, were where the proper combination of initial launch heading and turn rate resulted in the cross-plane angle ψ_V at burnout being equal to or near zero. As to which steering technique is the most efficient there appears to be little difference between the two. For the two values of offset investigated this minimum ΔV was found to be about 400 feet per second for the 2° offset and about 1,600 feet per second for the 4° offset as compared with 930 feet per second for the 2° offset and 1,960 feet per second for the 4° offset obtained by using the "adjacency" technique.

Langley Research Center,
National Aeronautics and Space Administration,
Langley Station, Hampton, Va., July 2, 1962.

APPENDIX A

DERIVATION OF EQUATIONS OF MOTION AND THRUST CONTROL EQUATIONS

Equations of Motion

The equations of motion were solved in an inertial right-handed system of axes x, y, and z with the origin at the center of a rotating spherical earth. The axes were oriented with the z-axis through the ascending node of the target orbit and the y-axis through the north pole. An auxiliary set of axes R, T, and N centered at the ferry vehicle's present position was also used. These axes were oriented such that the R,T plane lay in a plane that also passed through the ferry vehicle's present position and the ascending node of the target orbit with the T,N plane parallel to the plane of the local horizontal. The T-axis was in the direction of motion of the ferry vehicle. The two systems are shown in figure 1.

The transformation equation between the inertial and R,T,N axes is given by

$$\begin{vmatrix} (\ )x \\ (\ )y \\ (\ )z \end{vmatrix} = \begin{vmatrix} l_{11} & l_{12} & l_{13} \\ m_{21} & m_{22} & m_{23} \\ n_{31} & n_{32} & n_{33} \end{vmatrix} \begin{vmatrix} (\ )R \\ (\ )T \\ (\ )N \end{vmatrix} = A \begin{vmatrix} (\ )R \\ (\ )T \\ (\ )N \end{vmatrix} \tag{A1}$$

where terms substituted in the parentheses are quantities to be related to the proper axes.

The elements of the transformation matrix are:

$$l_{11} = \cos\theta \sin\Omega$$

$$l_{12} = \cos\delta \cos\Omega - \sin\delta \sin\theta \sin\Omega$$

$$l_{13} = \sin\delta \cos\Omega + \cos\delta \sin\theta \sin\Omega$$

$$m_{21} = \sin\theta$$

$$m_{22} = \sin\delta \cos\theta$$

$$m_{23} = -\cos\delta \cos\theta$$

$$n_{31} = \cos\theta \cos\Omega$$

$$n_{32} = -\cos\delta \sin\Omega - \sin\delta \sin\theta \cos\Omega$$

$$n_{33} = \cos\Omega \sin\theta \cos\delta - \sin\Omega \sin\delta$$

and θ, δ, and Ω are angles denoted in figure 1.

The basic equations of motion used for computation were:

$$m\ddot{x} = \bar{T}_x + W_x + D_x \tag{A2}$$

$$m\ddot{y} = \bar{T}_y + W_y + D_y \tag{A3}$$

$$m\ddot{z} = \bar{T}_z + W_z + D_z \tag{A4}$$

where $\bar{T}$, W, and D are the thrust, weight, and drag terms, respectively, and the subscripts denote components of these terms along the proper axes.

The R,T,N system of axes was used as a convenient reference for the vector quantities of thrust, drag (along V_a), and velocities V, V_a, and V_e. This system along with the vectors and the angles used to relate them to the system is shown in figure 1(b).

Thrust terms.- The components of thrust used in the equations are computed from the transformation (eq. (1)) and are

$$\begin{vmatrix} \bar{T}_x \\ \bar{T}_y \\ \bar{T}_z \end{vmatrix} = A \begin{vmatrix} \bar{T}_R \\ \bar{T}_T \\ \bar{T}_N \end{vmatrix} \tag{A5}$$

where, from figure 1(b),

$$\bar{T}_R = \bar{T} \sin\theta_T$$

$$\bar{T}_T = \bar{T} \cos\theta_T \cos\psi_T$$

$$\bar{T}_N = \bar{T} \cos\theta_T \sin\psi_T$$

and θ_T and ψ_T are the thrust control angles and can either be constants, or analytical or tabulated functions of time.

<u>Weight terms</u>.- The components of weight used in the equations were computed from the transformation and were in the form

$$\begin{vmatrix} W_x \\ W_y \\ W_z \end{vmatrix} = A \begin{vmatrix} -W \\ 0 \\ 0 \end{vmatrix} \tag{A6}$$

where W is the vehicle weight along the radius vector and is given by

$$W = mg_e \frac{(r_e)^2}{(r)^2} \tag{A7}$$

and

$$m = m_0 - \int \dot{m}\, dt$$

<u>Drag terms</u>.- The total drag D was assumed to act along the aerodynamic component of velocity V_a and is defined in these computations as

$$D = \frac{1}{2} \rho C_D S V_a{}^2$$

where V_a is the total aerodynamic velocity vector and is the vector sum of the components of V_a along the R, T, and N axes

$$V_a = \left(V_{a_R}{}^2 + V_{a_T}{}^2 + V_{a_N}{}^2\right)^{1/2}$$

where

$$V_{a_R} = V_R$$

$$V_{a_T} = V_T - V_e \cos \delta$$

$$V_{a_N} = V_N - V_e \sin \delta$$

and

$$\begin{vmatrix} V_R \\ V_T \\ V_N \end{vmatrix} = A^{-1} \begin{vmatrix} \dot{x} \\ \dot{y} \\ \dot{z} \end{vmatrix}$$

The components of drag used in the calculations were computed from the transformation, equation (A1), and are

$$\begin{vmatrix} D_x \\ D_y \\ D_z \end{vmatrix} = A \begin{vmatrix} D_R \\ D_T \\ D_N \end{vmatrix} \tag{A8}$$

where

$$D_R = -D \sin \zeta_{V_a}$$

$$D_T = -D \cos \zeta_{V_a} \cos \psi_{V_a}$$

$$D_N = -D \cos \zeta_{V_a} \sin \psi_{V_a}$$

Angular relationship and auxiliary terms.- The angles θ, Ω, and δ were computed in the following manner:

$$\theta = \sin^{-1}\left(\frac{y}{r}\right)$$

$$\Omega = \tan^{-1}\left(\frac{x}{z}\right)$$

$$\delta = \tan^{-1}\left(\frac{y}{x} \frac{z}{r}\right)$$

The inertial velocity angles were given as

$$\zeta_V = \sin^{-1}\left(\frac{V_R}{V}\right)$$

$$\psi_V = \sin^{-1}\left(\frac{V_N}{V \cos \zeta_V}\right)$$

The aerodynamic angles were given by

$$\zeta_{V_a} = \sin^{-1}\left(\frac{V_{a_R}}{V_a}\right)$$

$$\psi_{V_a} = \sin^{-1}\left(\frac{V_{a_N}}{V_a \cos \zeta_{V_a}}\right)$$

The offset angle η along the local meridian was defined as

$$\eta = \theta_p - \theta$$

where θ_p is the local latitude of a point in the target orbit and is given by the expression

$$\theta_p = \tan^{-1}\left(\frac{\sin \Omega \sin i_s}{\cos i_s}\right)$$

The offset distance d in feet is

$$d = \eta r$$

where η is in radians. Great circle range angle ϕ is given by

$$\phi = \tan^{-1}\left(\frac{+\left\{1 - \left[\sin \theta_0 \sin \theta + \cos \theta_0 \cos \theta \cos(\Omega - \Omega_0)\right]^2\right\}^{1/2}}{\sin \theta_0 \sin \theta + \cos \theta_0 \cos \theta \cos(\Omega - \Omega_0)}\right)$$

Initial heading of the thrust vector, ψ_{T_0}, is given by the following expression

$$\psi_{T_0} = H_0 - 90 + \delta_0$$

Derivation of Thrust Control Equations

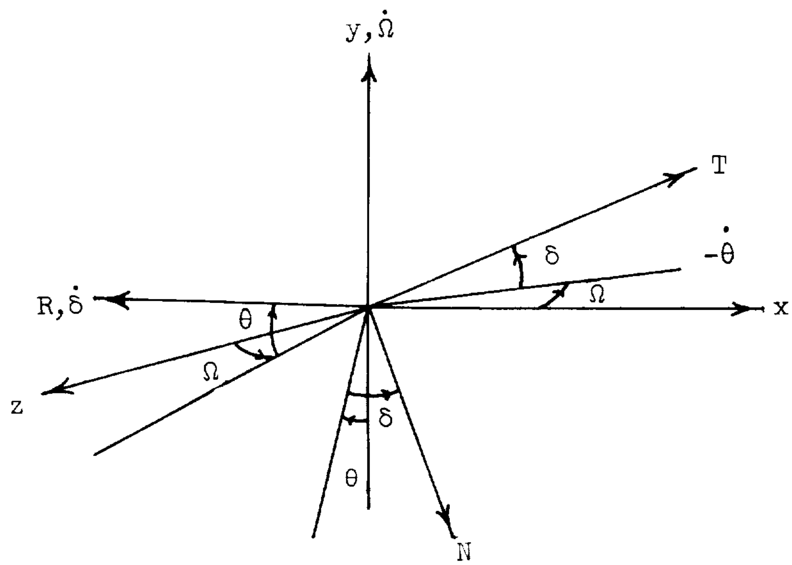

Sketch 4

The angular rates about the R, T, and N set of axes (sketch 4) due to Ω, θ, and δ rotations are

$$\omega_R = \dot{\delta} + \dot{\Omega} \sin \theta \tag{A9}$$

$$\omega_T = \dot{\Omega} \cos \theta \sin \delta - \dot{\theta} \cos \delta \tag{A10}$$

$$\omega_N = -\dot{\Omega} \cos \theta \cos \delta - \dot{\theta} \sin \delta \tag{A11}$$

For convenience, a new right-handed set of axes, x_B, y_B, and z_B, centered at the origin of the R,T,N systems of axes with the thrust vector parallel to the x_B-axis is presented (sketch 5) and because of ψ_T and θ_T rotations, in that order, the following equations result:

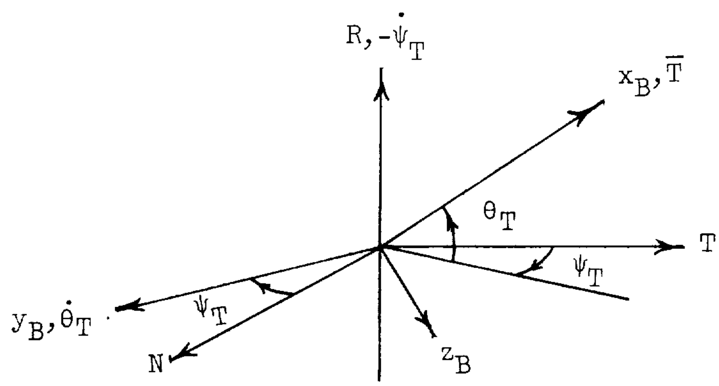

Sketch 5

$$\overline{\omega}_{x_B} = -\dot{\psi}_T \sin \theta_T \tag{A12}$$

$$\overline{\omega}_{y_B} = \dot{\theta}_T \tag{A13}$$

$$\overline{\omega}_{z_B} = \dot{\psi}_T \cos \theta_T \tag{A14}$$

where the bar denotes just those rates due to the θ_T and ψ_T rotations.

Defining the total rates about the x_B, y_B, and z_B axes as ω_{x_B}, ω_{y_B}, and ω_{z_B}, respectively, results in

$$\omega_{x_B} = -\dot{\psi}_T \sin \theta_T + f(\omega_R, \omega_N, \omega_T) x_B \tag{A15}$$

$$\omega_{y_B} = \dot{\theta}_T + f(\omega_R, \omega_N, \omega_T) y_B \tag{A16}$$

$$\omega_{z_B} = \dot{\psi}_T \cos \theta_T + f(\omega_R, \omega_N, \omega_T) z_B \tag{A17}$$

Resolving the components of ω_R, ω_T, and ω_N into components along the x_B, y_B, and z_B axes yields

$$\omega_{x_B} = -\dot{\psi}_T \sin \theta_T + \omega_R \sin \theta_T + \omega_T \cos \psi_T \cos \theta_T + \omega_N \sin \psi_T \cos \theta_T \tag{A18}$$

$$\omega_{y_B} = \dot{\theta}_T - \omega_T \sin \psi_T + \omega_N \cos \psi_T \tag{A19}$$

$$\omega_{z_B} = \dot{\psi}_T \cos \theta_T - \omega_R \cos \theta_T + \omega_T \cos \psi_T \sin \theta_T + \omega_N \sin \psi_T \sin \theta_T \tag{A20}$$

Combining equations (A9), (A10), and (A11) with equations (A18), (A19), and (A20) and eliminating the ω_{x_B} equation, since pitch- and yaw-rate equations are the only ones of interest, yields

$$\omega_{y_B} = \dot{\theta}_T - \dot{\Omega} \cos \theta \cos(\delta - \psi_T) - \dot{\theta} \sin(\delta - \psi_T) \tag{A21}$$

$$\begin{aligned} \omega_{z_B} = \left(\dot{\psi}_T - \dot{\delta}\right)\cos \theta_T + \dot{\Omega}\Big[\sin \theta_T \cos \theta \sin(\delta - \psi_T) \\ - \cos \theta_T \sin \theta\Big] - \dot{\theta} \sin \theta_T \cos(\delta - \psi_T) \end{aligned} \tag{A22}$$

Solving for $\dot{\theta}_T$ and $\dot{\psi}_T$ in equations (A21) and (A22) and collecting terms yields

$$\dot{\theta}_T = \omega_{y_B} + \dot{\theta} \sin(\delta - \psi_T) + \dot{\Omega} \cos \theta \cos(\delta - \psi_T) \tag{A23}$$

$$\begin{aligned} \dot{\psi}_T = \frac{\omega_{z_B}}{\cos \theta_T} + \dot{\delta} + \dot{\Omega}\Big[\sin \theta - \tan \theta_T \cos \theta \sin(\delta - \psi_T)\Big] \\ + \dot{\theta} \tan \theta_T \cos(\delta - \psi_T) \end{aligned} \tag{A24}$$

From figure 1(a) it can be seen that

$$r\dot{\theta} = -V_N \cos\delta + V_T \sin\delta$$

Hence

$$\dot{\theta} = -\frac{V_N \cos\delta + V_T \sin\delta}{r} \tag{A25}$$

and

$$r \cos\theta\dot{\Omega} = V_T \cos\delta + V_N \sin\delta$$

Hence

$$\dot{\Omega} = \frac{V_T \cos\delta + V_N \sin\delta}{r \cos\theta} \tag{A26}$$

Differentiating the equation

$$\tan\delta = \frac{\sin\theta}{\tan\Omega}$$

and making use of certain trigonometric identities and equations (A25) and (A26) yields

$$\dot{\delta} = -\frac{\cos\delta}{r\cos\theta}\left(\frac{V_N \tan\delta}{\sin\theta} + V_T \sin\theta\right) \tag{A27}$$

By substitution of equations (A25), (A26), and (A27) into equations (A23) and (A24) and collecting terms, the thrust control equations become simply

$$\dot{\theta}_T = \omega_{y_B} + \frac{1}{r}\left(V_T \cos\psi_T + V_N \sin\psi_T\right) \tag{A28}$$

$$\dot{\psi}_T = \frac{\omega_{z_B}}{\cos\theta_T} + \frac{1}{r}\left[V_T \tan\theta_T \sin\psi_T - V_N\left(\frac{\sin\delta}{\tan\theta} + \tan\theta_T \cos\psi_T\right)\right] \tag{A29}$$

REFERENCES

1. Bird, John D., and Thomas, David F., Jr.: A Two-Impulse Plan For Performing Rendezvous on a Once-A-Day Basis. NASA TN D-437, 1960.

2. Houbolt, John C.: Considerations of the Rendezvous Problems for Space Vehicles. Preprint No. 175A, Soc. Automotive Eng., Apr. 1960.

TABLE I.- SUMMARY OF LAUNCH TRAJECTORY CONDITIONS AND THE IDEALIZED VELOCITY INCREMENT REQUIRED FOR FINAL RENDEZVOUS

Case	Initial heading, deg	Turn rate, deg/sec	ζ_V, deg	ψ_V, deg	V_f, 1/sec	ΔV, 1/sec
Constant-rate method; $\eta_O = 2^\circ$						
0	86.64	0	0.362	5.489	25,472	2,446
1	86.74	-.004	.361	5.249	25,471	2,339
2	87.64	-.039	.302	2.356	25,367	1,061
3	88.40	-.065	.178	.065	25,142	358
Fixed-direction method; $\eta_O = 2^\circ$						
4	87.54	-5.00	0.377	4.067	25,436	1,816
5	88.40	-9.40	.324	2.706	25,362	1,216
6	89.24	-13.80	.235	1.341	25,231	656
7	90.04	-16.90	.128	.161	25,087	412
Constant-rate method; $\eta_O = 4^\circ$						
0	87.40	0	0.372	11.274	25,473	5,009
1	88.30	-.038	.314	8.339	25,380	3,703
2	89.90	-.097	.020	3.492	24,801	1,680
3	91.10	-.137	-.472	0	24,061	1,444
Fixed-direction method; $\eta_O = 4^\circ$						
4	88.3	-5.15	0.383	9.885	25,440	4,392
5	89.9	-13.00	.263	7.480	25,282	3,330
6	94.4	-34.5	-.686	.637	23,948	1,594

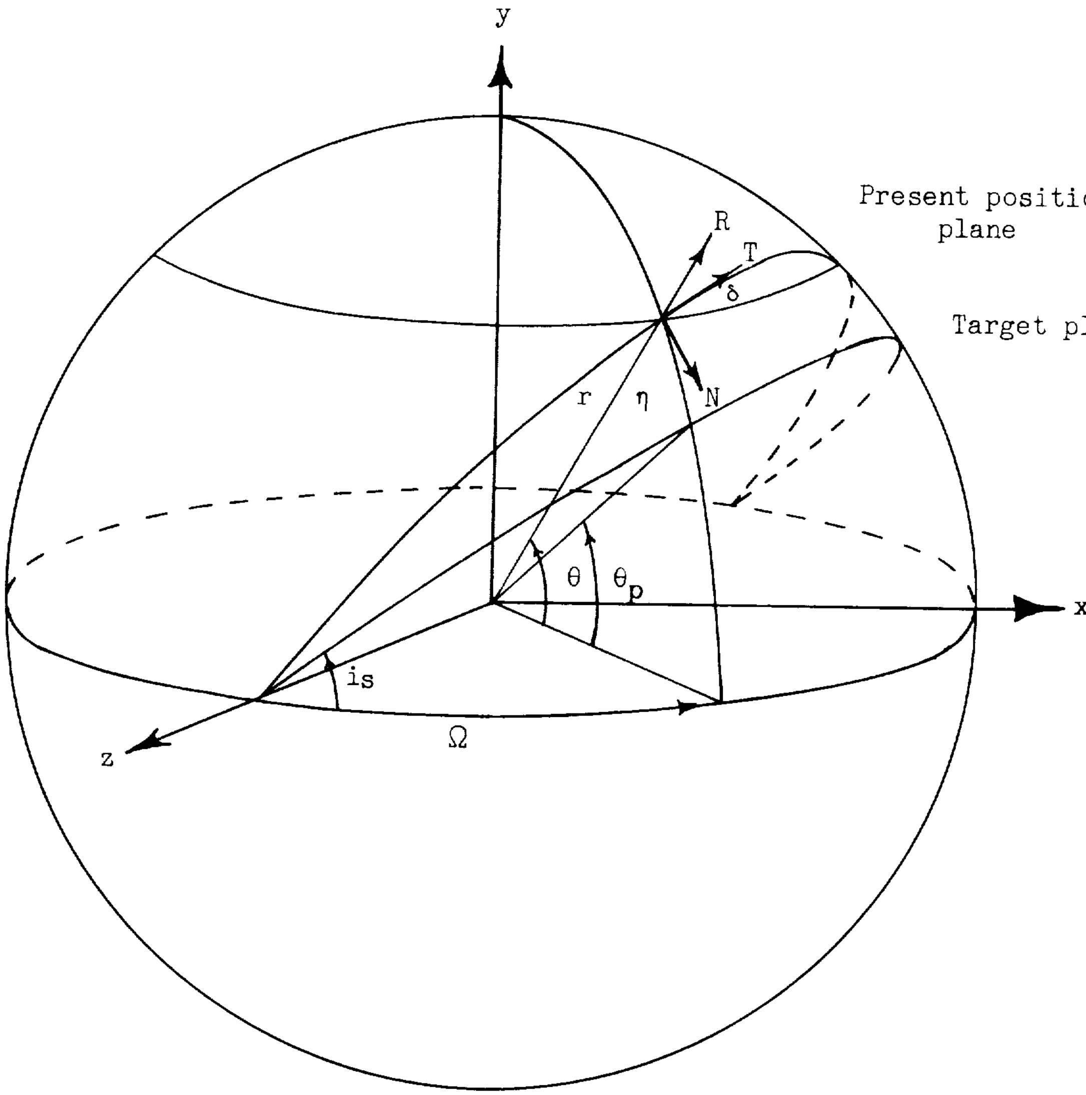

(a) Trajectory coordinates.

Figure 1.- Coordinate systems and notation.

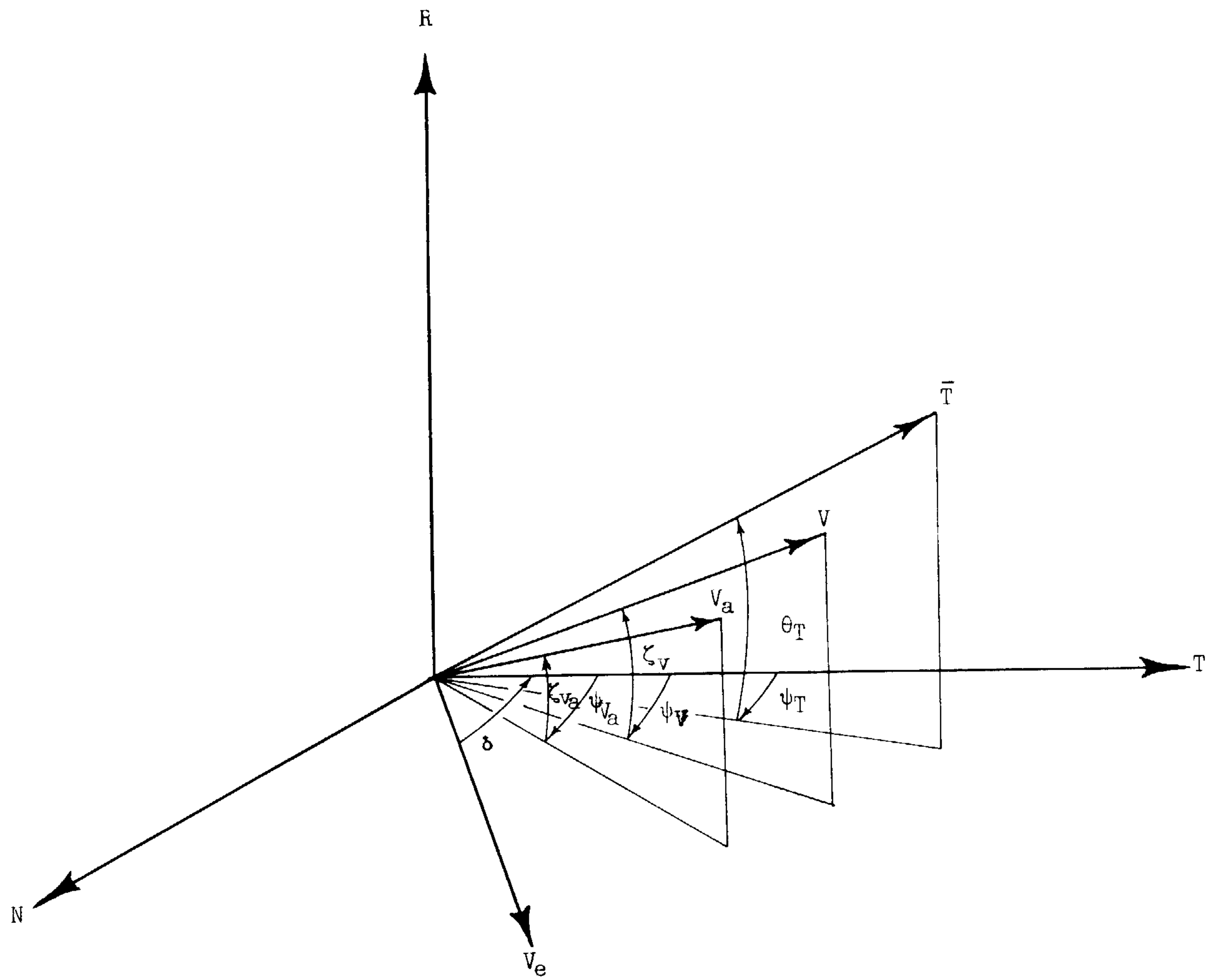

(b) The R,T,N system of axes.

Figure 1.- Concluded.

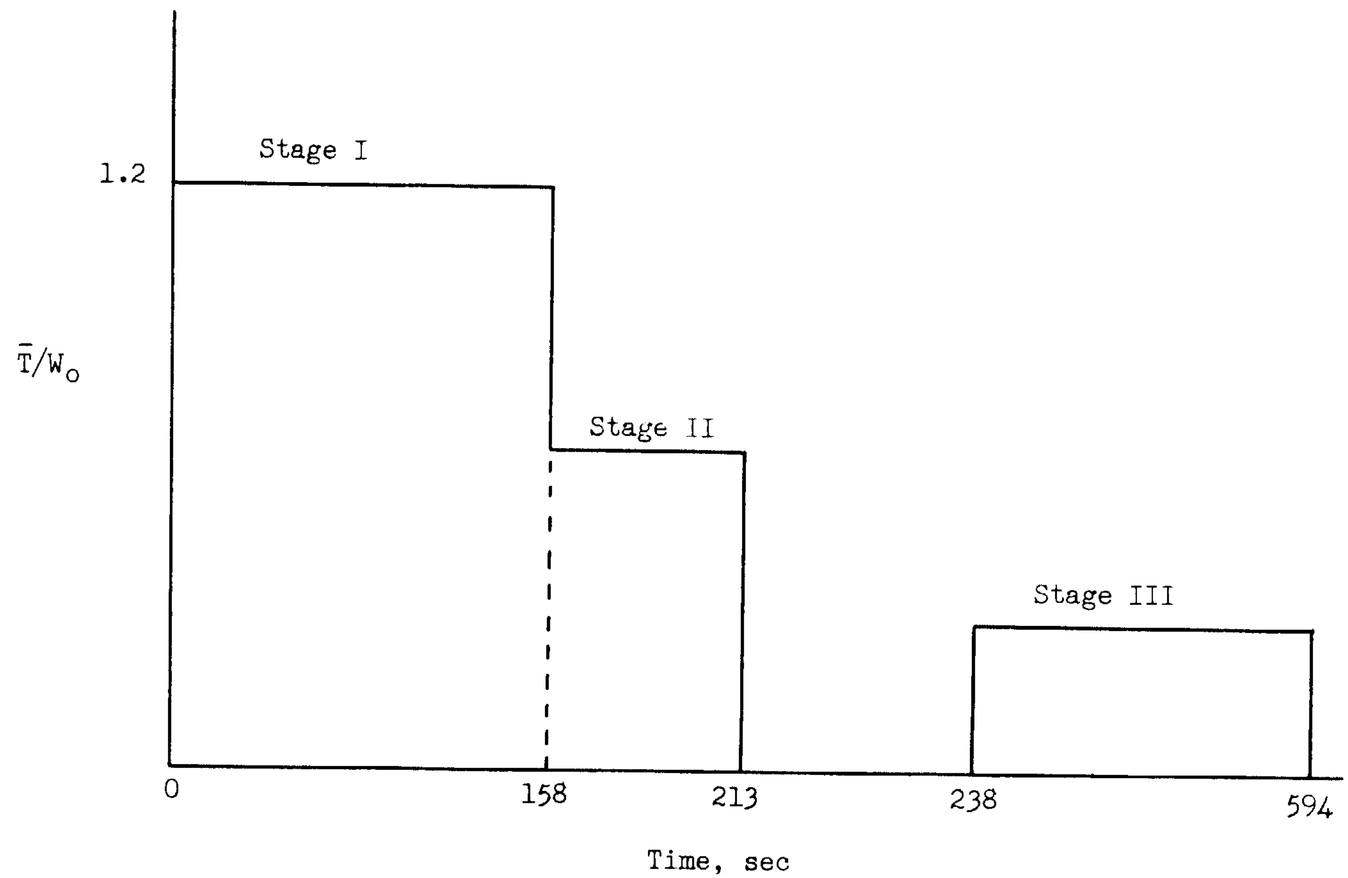

Figure 2.- Thrust profile of the launch vehicle and staging times.

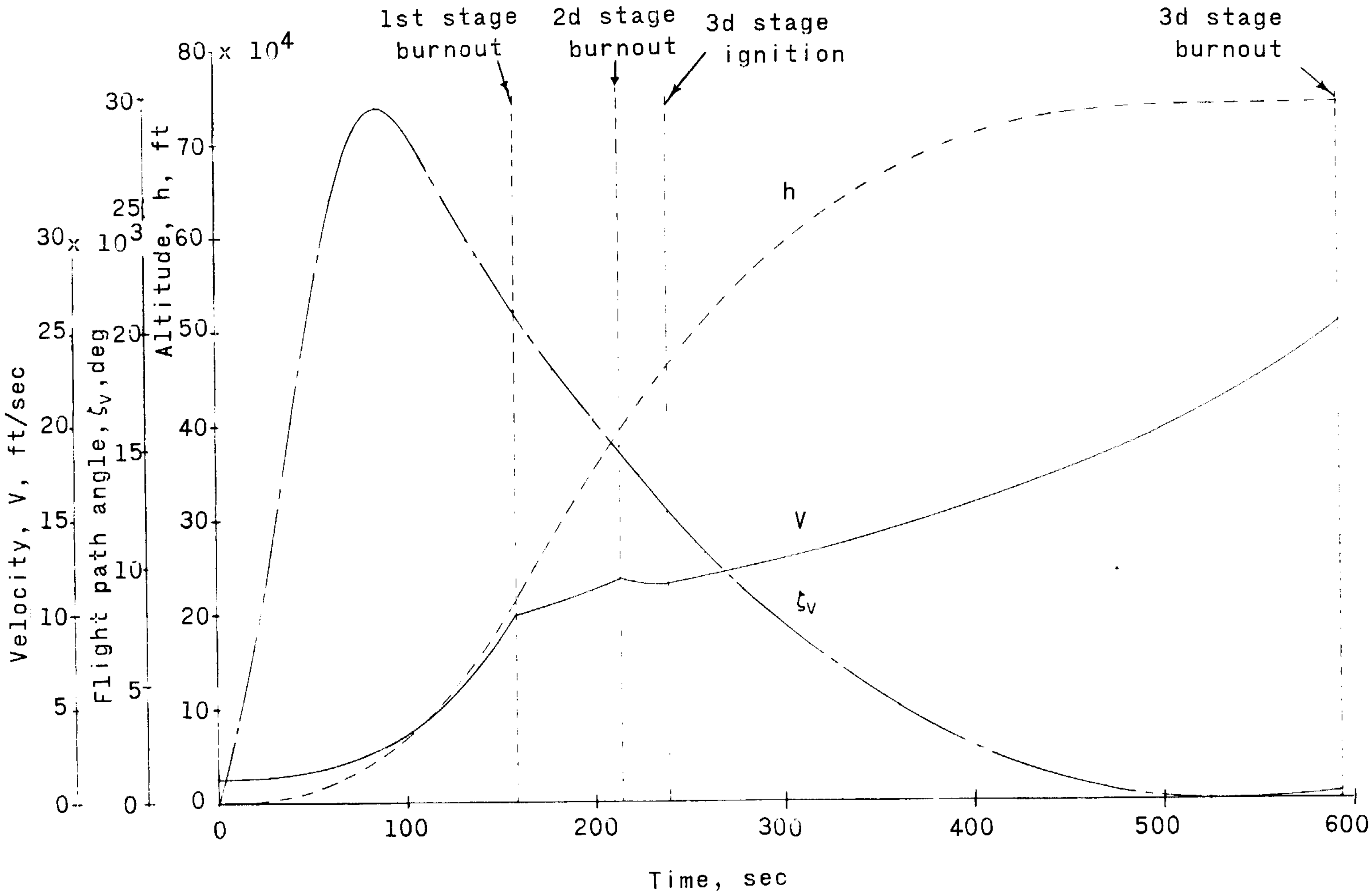

Figure 3.- Inertial velocity, flight angle, altitude, and time histories for the basic launch trajectory.

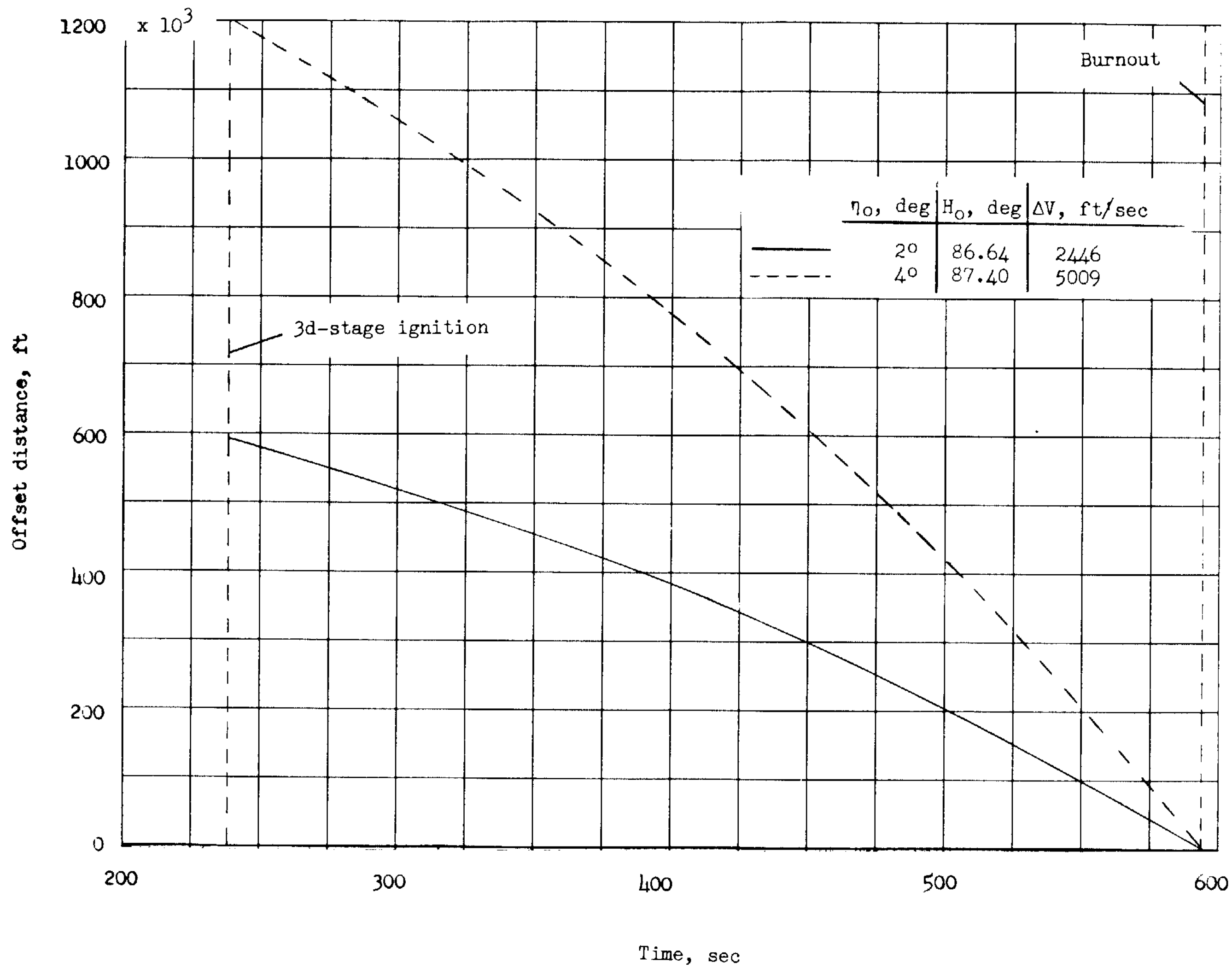

Figure 4.- Offset-distance time history for the straight-in (no turn) cases for $\eta_O = 2^\circ$ and 4°.

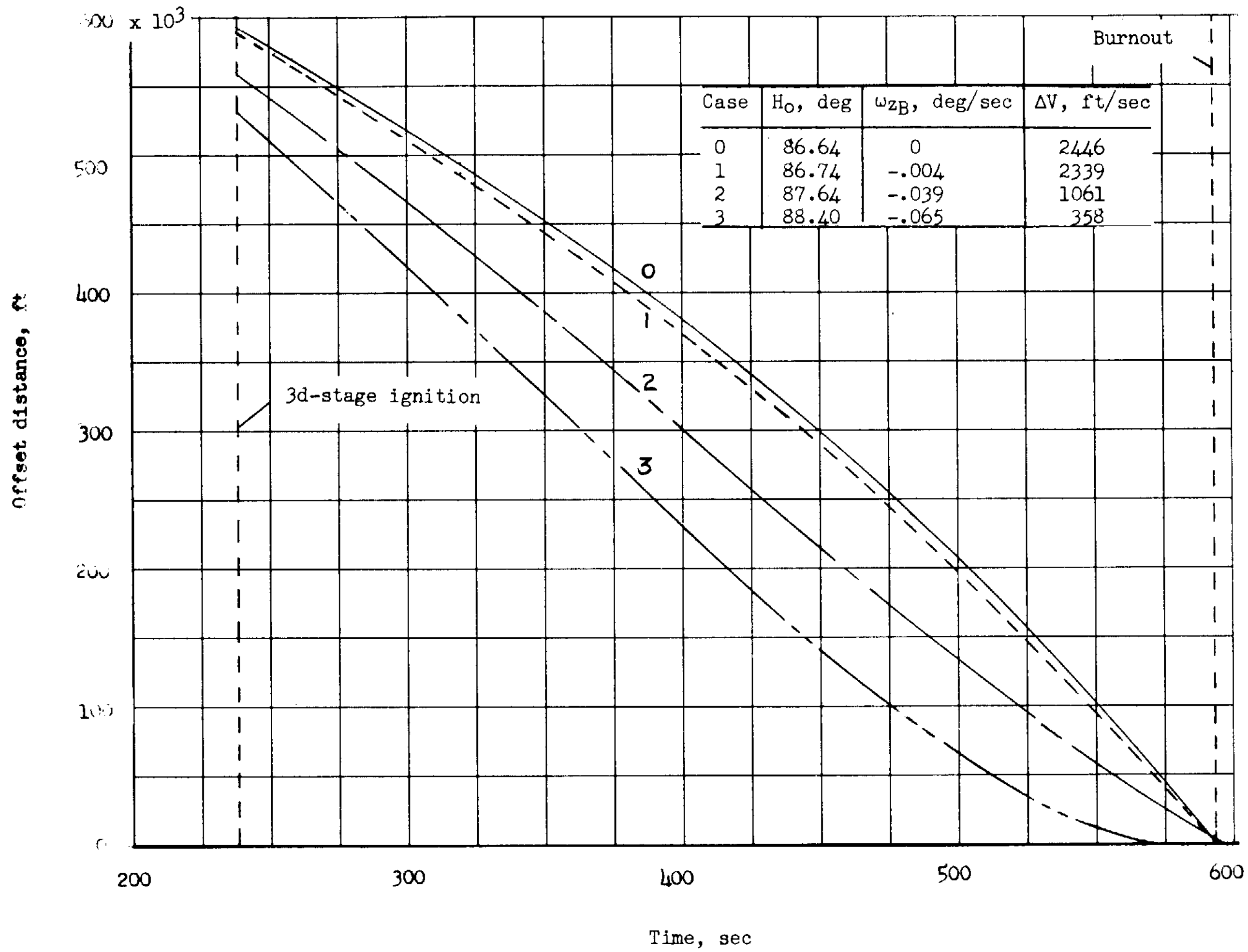

(a) Constant-rate method.

Figure 5.- Offset-distance time history for $\eta_0 = 2^{\circ}$.

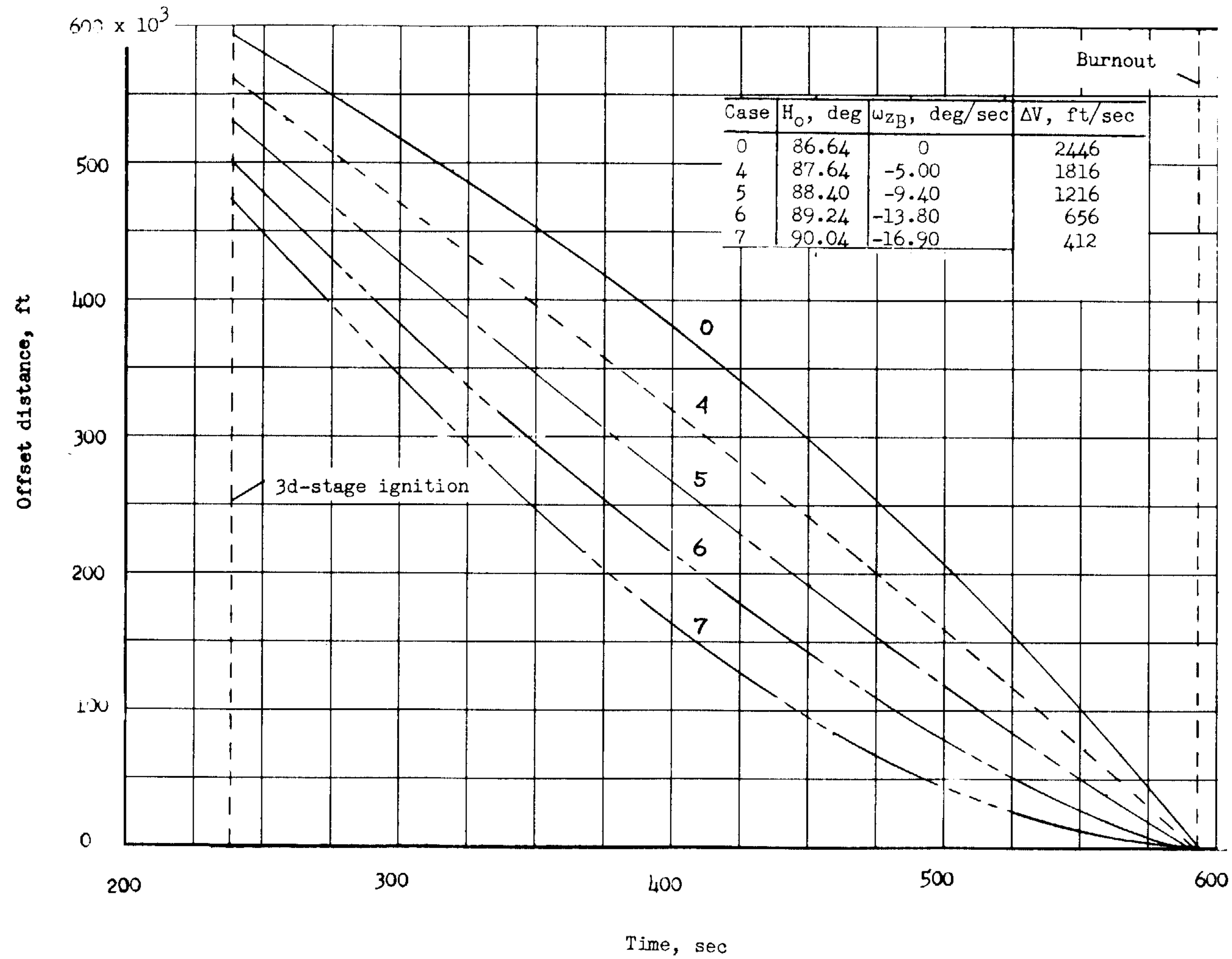

(b) Fixed-direction method.

Figure 5.- Concluded.

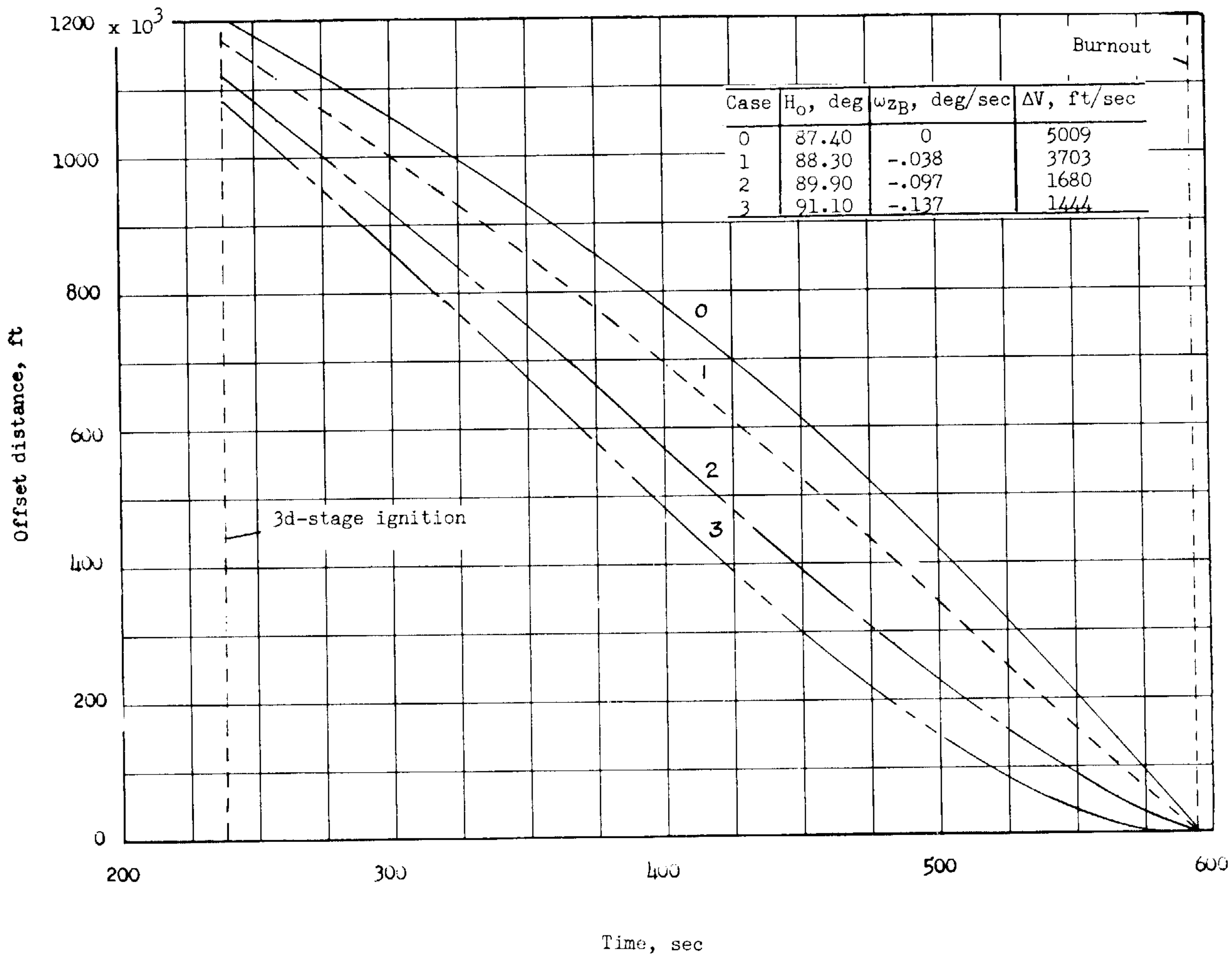

(a) Constant-rate method.

Figure 6.- Offset-distance time history for $\eta_0 = 4^{\circ}$.

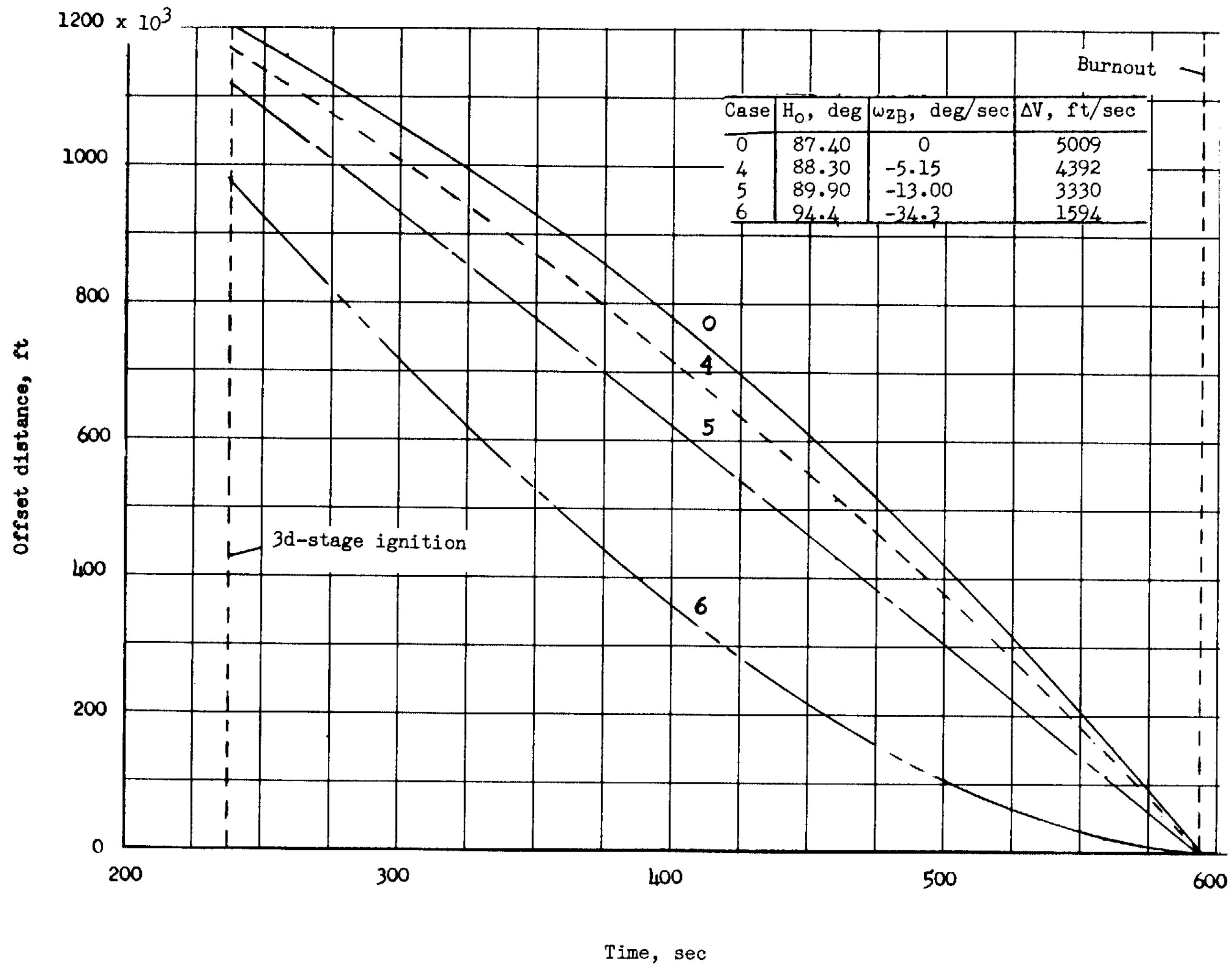

(b) Fixed-direction method.

Figure 6.- Concluded.

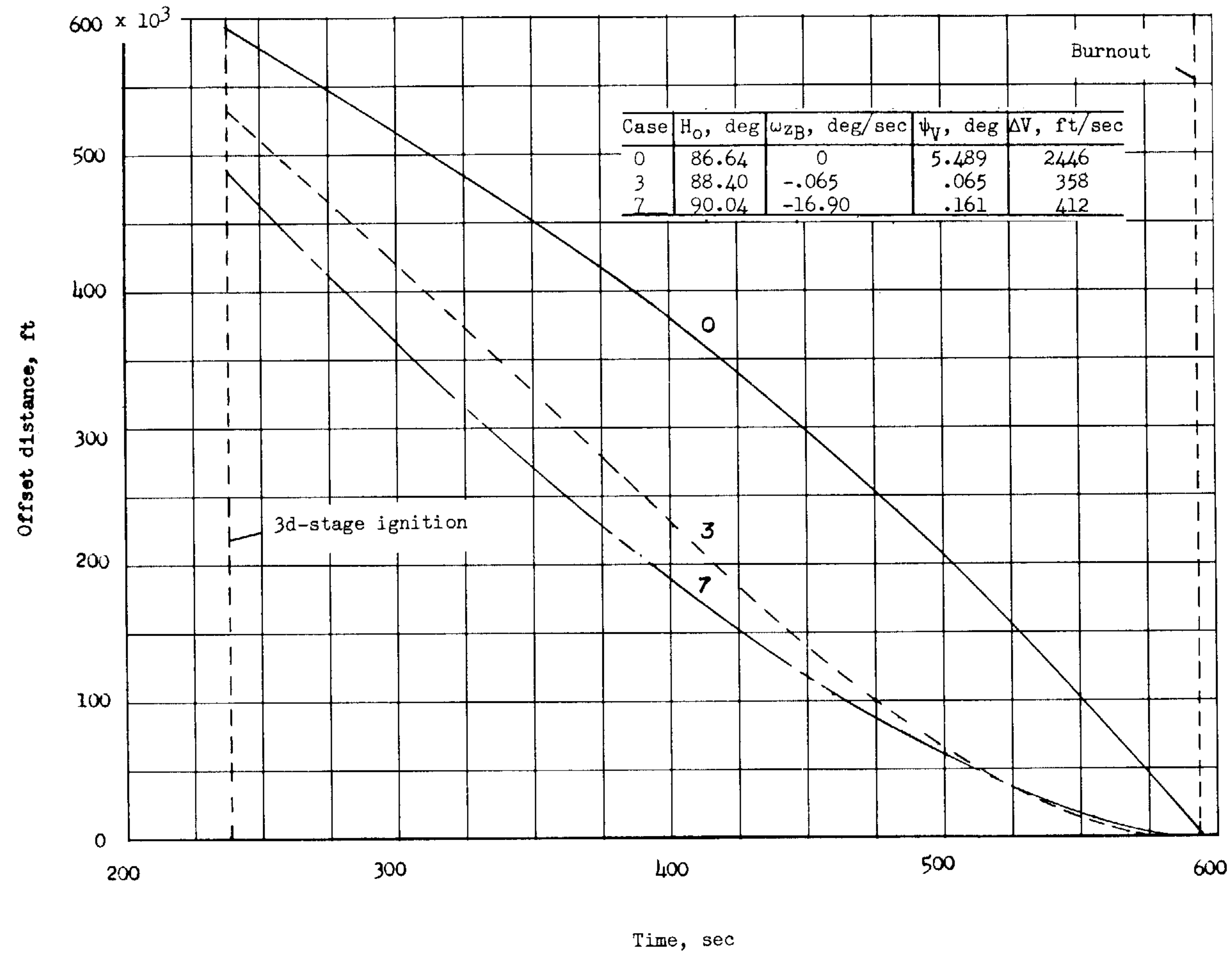

Case	H_o, deg	ω_{z_B}, deg/sec	ψ_V, deg	ΔV, ft/sec
0	86.64	0	5.489	2446
3	88.40	-.065	.065	358
7	90.04	-16.90	.161	412

(a) $\eta_0 = 2^{\circ}$.

Figure 7.- Offset-distance time history for the cases that resulted in the cross-plane angle, ψ_V, at burnout approximately equal to zero for both steering techniques.

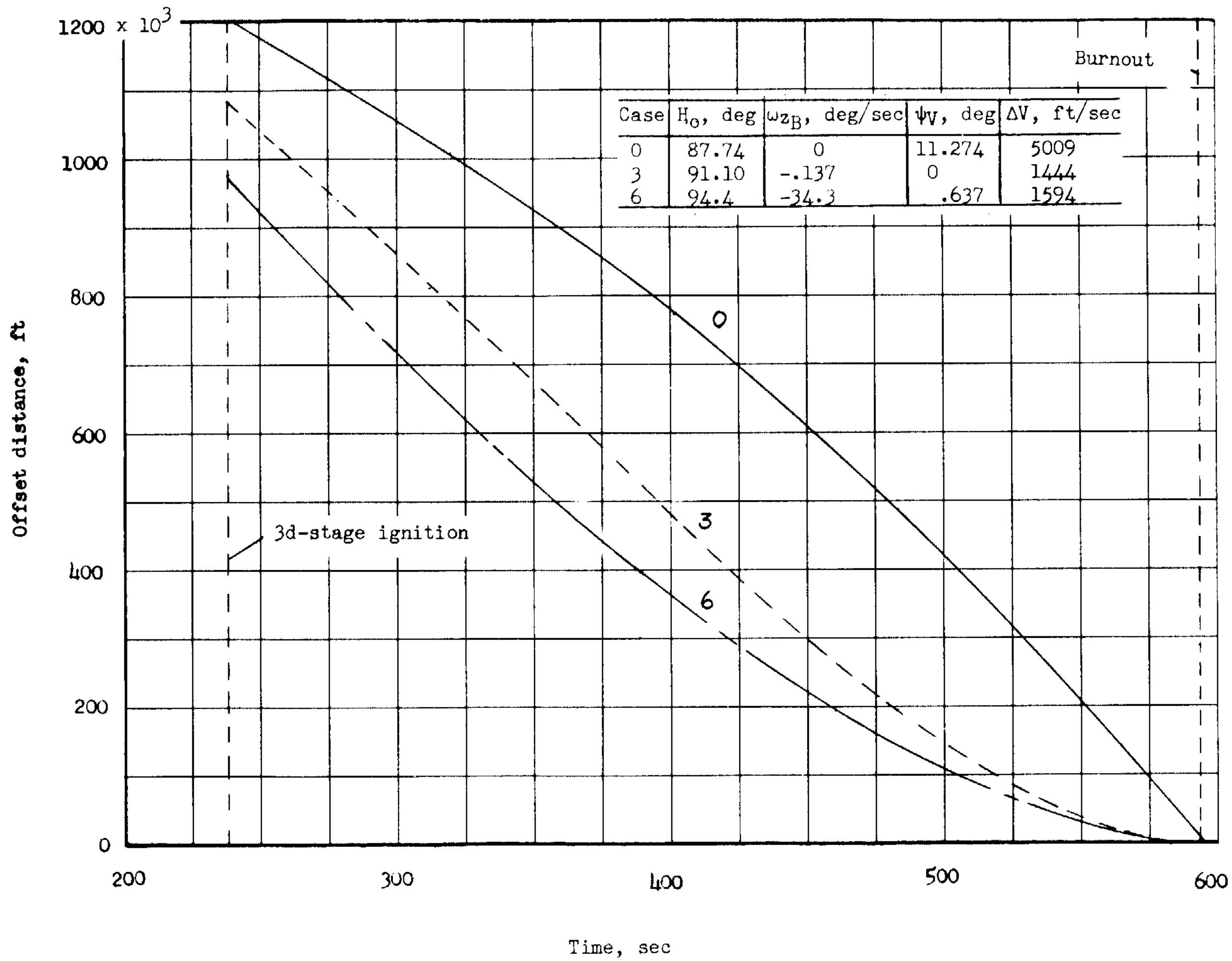

Case	H_o, deg	ω_{z_B}, deg/sec	ψ_V, deg	ΔV, ft/sec
0	87.74	0	11.274	5009
3	91.10	-.137	0	1444
6	94.4	-34.3	.637	1594

(b) $\eta_0 = 4^{\circ}$.

Figure 7.- Concluded.

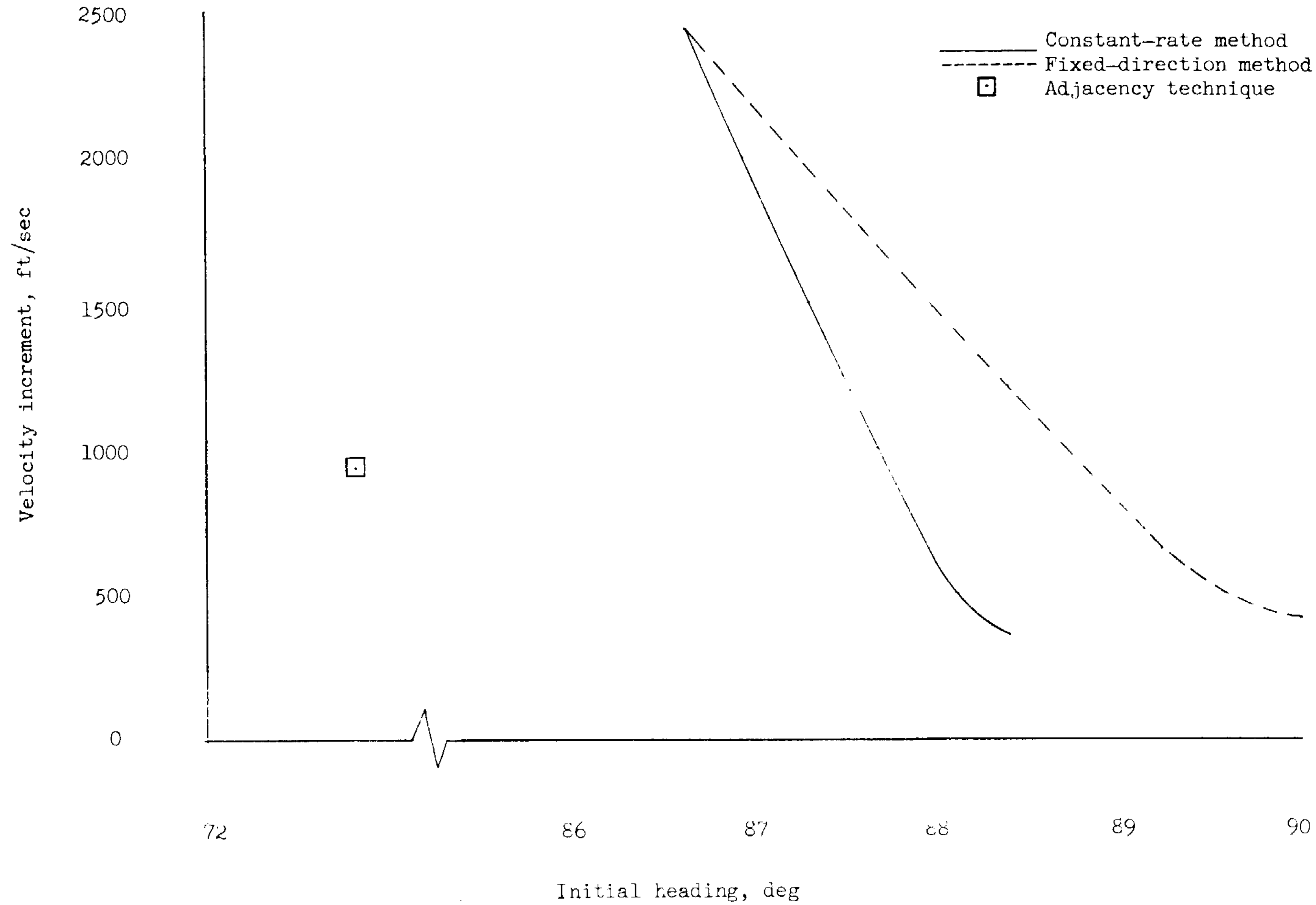

(a) $\eta_0 = 2^{\circ}$.

Figure 8.- Idealized velocity increment ΔV required to initiate final rendezvous as a function of initial launch heading.

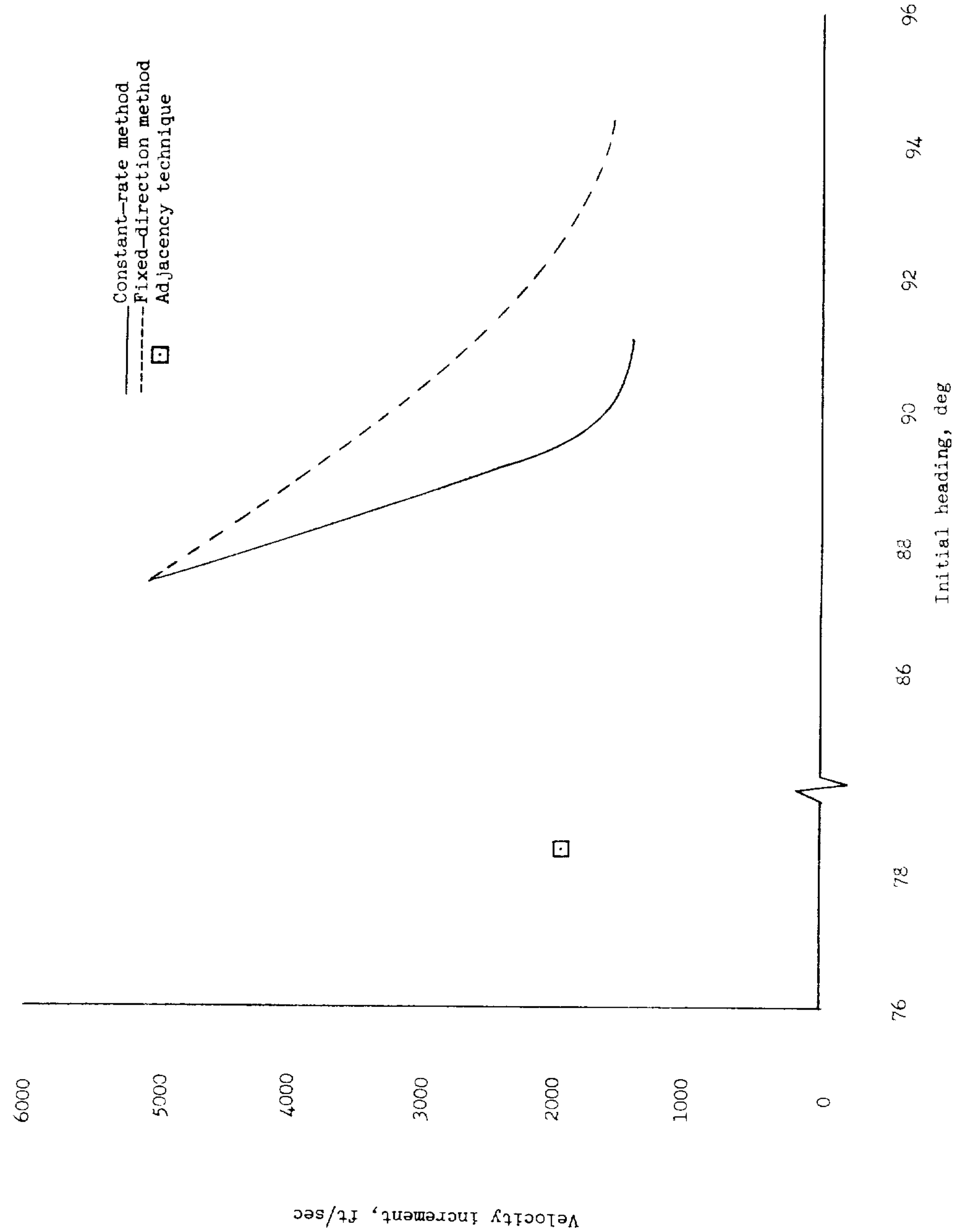

(b) $\eta_0 = 4^{\circ}$.

Figure 8.- Concluded.